Proposal of a Novel Design for Linear Superconducting Motor Using 2G Tape Stacks

G. G. Sotelo[1,2], F. Sass[1], M. Carrera[3], Josep Lopez-Lopez[4], X. Granados.[2]

[1] Electrical Engineering Department, Fluminense Federal University (UFF), Niterói - Brazil

[2] Institut de Ciències de Materials de Barcelona (ICMAB CSIC), Barcelona - Spain

[3] Dep. Medi Ambient i Ciències del Sòl, Universitat de Lleida (UdL), Lleida - Spain

[4] Universitat Politècnica da Catalunya (UPC), Barcelona - Spain

***Abstract*—This manuscript presents a new design for superconducting linear motor (SLM). This SLM uses stacks of second generation (2G) superconducting tapes, which are responsible for replacing YBCO bulks. The proposed SLM may operate as a synchronous motor or as a hysteresis motor, depending on the load force magnitude. A small scale linear machine prototype with 2G stacks was constructed and tested to investigate the proposed SLM topology. The stator traveling magnetic field wave was represented by several Nd-Fe-B permanent magnets. A relative movement was produced between the stator and the stack, and the force was measured along the displacement. This system was also simulated by finite element method, in order to calculate the induced currents in the stack and determine the electromagnetic force. The H-formulation was used to solve the problem and a power law relation was applied to take into account the intrinsically nonlinearity of the superconductor. The simulated and measured results were in accordance. Simulated results were extrapolated, proving to be an interesting tool to scale up the motor in future projects. The proposed motor presented an estimated force density of almost 500 N/kg, which is much higher than any linear motor.**

***Index Terms*— Linear motors, Superconducting machine, Superconducting modeling.**

I. Introduction

SUPERCONDUCTING second generation (2G) tapes are manufactured by depositing a RE-Ba-Cu-O (where RE is a rare earth material) ceramic layer of 1~2 μm thickness above a metallic substrate. Commercial 2G tapes with 12 mm wide and a total thickness of 0.1 mm can present a critical current of 600 A at 77 K and self-field[1,2,3]. Those properties make the 2G tapes a promising material to be used in power electric equipment, including electric machines. Several designs of superconducting motors and generators have been previously presented in the literature [1-3]. In most part of the published works the superconducting material was arranged in the form of coils; however, bulk superconductor with trapped field can also be used for electric machines [4-6]. Stacks of 2G tapes have been proposed as a potential substitute of bulk superconductors [7-9]. The literature also presents the 2G tapes stacks in several different applications, like: cables [10-13], rotational electric machines [14-15], superconducting levitation [16-19], etc. The advantages of 2G tapes in relation with bulks are its higher robustness, the ability to transport high electric current, the number of available manufacturers and large scale production.

A novel type of linear superconducting motor using 2G tape stacks is proposed in the present manuscript. The understanding of this motor can be simplified by the schematic shown in Fig. 1. A three phase stator is responsible to produce a traveling magnetic field, as described in the basic books of electric machines [20]. Magnetic field is trapped in the pinning centers of the superconductor stack. At synchronous speed (v_s) the stack follows this field due to the pinning forces, producing a force in the same direction of the movement, named here as $F_{pinning}$. If a mechanical load is connected to the stack, a load force (F_{load}) appears in the opposite direction of the traveling magnetic field wave. If $F_{pinning} > F_{load}$, the stack will move in the synchronous speed and the motor operates as a synchronous machine. However, if $F_{pinning} < F_{load}$, there is a slip and the stack moves slower than v_s. In this case the traveling field leads the superconductor to a hysteresis cycle and due to it the machine is named as hysteresis motor. In the case of hysteresis operation mode, there are losses produced by the hysteresis cycle.

Below its critical temperature (T_c = 92 K), the easiest way to cool down the superconductor is using liquid nitrogen. In the

1- http://i-sunam.com/home/en_product,1,3,1,1,1
2- http://www.superpower-inc.com/
3- http://www.superox.ru/en/products/974-vtspprovod/

case of a linear motor for practical application, the stack must work inside a cryostat with a vacuum chamber. A similar kind of cryostat was designed for MagLev vehicles using superconducting linear bearings [21]. The proposed cryostat for the superconducting motor is presented in Fig. 2 (a). The cover has two through tubes for inlet and outlet of liquid nitrogen into the vessel. The mechanical load is connected at the top of this cover. Fig. 2 (b) presents a schematic with a section of the three phase stator, which has its windings Y connected. When these windings are fed by a three phase power source, a magnetic field traveling wave is produced in the gap region, where the lower part of the cryostat with the superconducting 2G stack is positioned, as presented by Fig. 2(c). In this illustration, three stacks made of 2G tapes were assembled in the cryostat. This type of linear motor was not previously presented in the literature.

In this context, this paper presents a new concept of superconducting linear motor using 2G tapes stacks. The motor performance was evaluated by investigating the traction force. A small scale test bench was built for experimental measurements and the problem was modelled in terms of the finite element method using the H formulation. In order to take into account nonlinearities inherent to the superconducting materials, the power law was used to model the superconductor behavior [22-24]. The small scale linear superconducting electric motor test bench is composed by a flat 2G tape stack with 9 layers and a stator with Nd-Fe-B magnets, which produces the external magnetic field.

The formulation used here can be extrapolated to scale up the motor. Based in this simple experiment, some contributions can be highlighted, such as: to prove the feasibility of superconducting linear machines using 2G tape stacks, to investigate the physical principles involved in the problem, and to test a model for future design of synchronous and hysteresis linear electric machines.

II. THE EXPERIMENTAL RIG

In order to estimate the torque of a superconducting electric machines operating with stacks of 2G tapes, a simple experiment set up was designed to represent a linear machine. This system is composed by two iron strips, Nd-Fe-B magnets and a 2G tape stack, presented and schematized in Fig. 3. The external magnetic field that is applied to the 2G tape stack is produced by a magnetic system composed by six pairs of Nd-Fe-B magnets (N38 type) that configure an alternate magnetic field in the gap. Each magnet is 20 mm long, 10 mm wide and 5.0 mm thick. The gap between magnets has 4.0 mm, and it is where the magnetic interaction occurs: the magnetic channel (MC). The system allows the stacks of superconducting tapes to move vertically through the MC.

The stack used in this work is presented in Fig. 4. It was manufactured with 9 pieces of SF12050-AP 2G HTS tape produced by SuperPower in 2013. The 2G tape has an average critical current and *n* exponent at self-field and liquid nitrogen (LN2) of 281 A and 35, respectively in self field conditions. The stack has the following dimensions: 12 mm width, 510 μm thickness and 30 mm length. During the stack production, epoxy resin was applied among each 2G HTS tape layer and the system was placed in a press in order to remove the adhesive excess and to minimize its thickness.

The transverse magnetic induction was measured in the MC using a proprietary Hall probe scanning microscopy. The result of the transversal measured magnetic flux density in the MC is presented in Fig. 5. During the measurements, the sensor was positioned at a fixed *y* coordinate equal to 0 mm, just centered in the MC (Fig. 3).

The experimental rig designed to measure the force between the stack and the permanent magnets has three parts well defined, which are indicated in Fig. 6: (A) Cryogenic deposit with magnets that create the magnetic field distribution and generate the forces; (B) Block that performs a displacement of the superconducting tapes in vertical direction; (C) Force sensors capable to measure the vertical force applied over the superconducting tape.

The part “A” of the experimental system setup (see Fig. 7) is composed by a cylindrical brass reservoir (1) having 110 mm diameter and 230 mm height, filled with LN_2. The deposit can be moved up or down to immerse the magnets (5) in LN_2 or leave them at room temperature. A stainless steel (AISI 316) cylindrical tube (2) has one of its terminals connected to the bench and the other is attached to a copper press (3), which holds a thin steel plate (4) that is connected to the magnet system (5) in a fixed vertical position.

In this system, it is possible to perform field cooling (FC) or zero field cooling (ZFC) tests indistinctly, just changing the initial relative stack position during the cooling down process.

The part “B” of the system is a set of two stepper motors that move the superconducting stack vertically at constant velocity, while the force is measured continuously. An Arduino® microcontroller was used to control the 2G tape stack position and speed. A range of velocities between 0.061 mm s^{-1} and 0.334 mm s^{-1} were explored.

The force applied over the stack is measured (part “C” of the system) using a load cell Utilcell Dat-400. This cell can be adjusted to not take into account the weight of the tape. The resolution of the load cell is lower than 0.20 g. Labview software was used to acquire the force and the position of the system. The force measurement results will be further presented.

III. MODELING THE PROPOSED PROBLEM

The system presented in the previous section was modeled by the H-formulation. The H-formulation has been applied in several works to calculate the current distribution in 2G tapes [22-24]. The small scale superconducting machine was modeled in 2D following the same procedures described in [25-26]. A constraint was defined to force a closed current loop, keeping the net

current equal to 0 ($I_{net.} = \int JdS = 0$). The Faraday's law $\left(\nabla \times \boldsymbol{E} = -\mu \frac{\partial \boldsymbol{H}}{\partial t}\right)$, for 2D symmetry systems leads to the following partial differential equations: $\mu \frac{\partial H_x}{\partial t} + \frac{\partial E_z}{\partial y} = 0$ and $\mu \frac{\partial H_y}{\partial t} - \frac{\partial E_z}{\partial x} = 0$.

Using the Ampere's law for low frequencies (J=∇×H), neglecting the displacement current, the relation between the current density inside the superconductor and the magnetic field can be obtained, as $J_z = \frac{\partial H_y}{\partial x} - \frac{\partial H_x}{\partial y}$.

The constitutive relation between the electric field and the current density is stablished in the HTS domains:

$$E_z = J_z \cdot \rho(J_z) = J_z \cdot \frac{E_c}{J_c} \left|\frac{J_z}{J_c}\right|^{n-1}, \qquad (1)$$

where ρ is highly non-linear, E_c is commonly adopted as 1 μV/cm, and the critical current density J_c and n are functions that can be obtained by the 2G tape manufacturer for a specific sample. Furthermore, the n exponent is field dependent with B, and this relation was considered using a curve obtained from a similar material, as done in [26]. This approach can be used for magnetic inductions in the range of 0-1T, presenting n = 20~25 at 77 K [27]. The above equations were solved by COMSOL® software using the finite element method (FEM). Additionally, rotational first order edge elements were used to reach a faster convergence of the partial differential equations.

As presented in Fig. 8(a), the experimental rig was modeled in 2D using a reduced domain, which can be seen in more details in Fig. 8(b). In order to do that, the magnetic field at the boundary conditions of the simulation domain must be computed at each time step and applied as Dirichlet boundary condition. In the domain boundaries, the magnetic field has an external (*ext*) component produced by the permanent magnets outside the simulation domain, and a component due to the induced currents in the superconductors (*HTS*) [25].

The applied external field was computed by analytical equations, considering two opposites current layers for each permanent magnet, such as done in [25]. The 12 permanent magnets were modeled analytically (applying the Biot-Savart's law) by the current surfaces presented in Fig. 8, and the respective magnetic induction was considered in the external boundary of the computing domain. Here, the soft ferromagnetic material was not represented in the formulation; however the simulated magnetic flux density results were adjusted to fit with the measurements of Fig. 5 by increasing the thickness and the current for each magnet. The comparison between the simulated and measured results is presented in Fig. 9 after adjustments.

To simulate the relative movement between the 2G tape stack and the external field, a linear constant speed function with the time was inserted in the magnetic induction profile presented in Fig. 9. During this movement, currents are induced in the 2G stack region as a solution of the problem. Finally, the force can be calculated by the Lorentz's force equation.

Table I presents the parameters used to simulate the 2G tapes and the HTS stack. The superconductor material was approximated as an isotropic material, and the critical current density dependency with the applied field was obtained by the manufacturer measurements. The same procedure was successfully applied in previous work [26]. The simulated results will be compared with the measured ones in the next section.

IV. Measured and Simulated Results

The simulations and measurements were performed using the procedures described in the two previous sections. Here, the homogenization technique of the 2G tape stack was used [24], considering 1, 3 and 9 domains for comparison. It was applied a constraint in each domain forcing the net current in the superconducting domain to be zero. Since the homogenization technique changes the superconductor cross-sectional area, the engineering critical current density has been used. The comparison between measured and simulated force results for two constant speeds (0.344 mm/s and 0.207 mm/s) are presented in Figs. 10 and 11. Those results were made for the FC case, with the left side of the stack in the middle of magnets 1 and 7 (Fig. 8), and with the parameters presented in Table I. It can be observed from Figs. 10 and 11 that the averaged force density over the displacer is about 5000 N/kg, only considering the stack mass.

In order to show the potential of this technology, Table II presents the force density results for several motors with data obtained from the literature, considering only the displacer mass. To make this comparison more realistic, the displacer force and force density are estimated for the HTS 2G stack motor, including the mass of other materials used in this displacer. The estimation is made based in the didactic illustration presented in Fig. 2, having 308 mm length. An estimated force for this motor is 2240 N, obtained from extrapolation of measured results, considering the displacer with 3 stacks in parallel having 90 2G HTS tape pieces each.

The calculated displacer mass is 4.5 kg, considering G10 as the cover plate, stainless steel for the cryostat external wall and copper for the heat transfer material. The force density in the proposed motor is much higher than in all other presented technologies. For those simulations, a personal computer with the following specifications was used: processor i7, clock 3.9 GHz and memory RAM of 16 Gb. The FEM mesh in the superconducting region was made with rectangular elements. It had 50 divisions along the 30 mm length, and along the thickness. The number of divisions was changed in accordance with the number of domains adopted: 3 divisions along the thickness for 1 and 3 domains, and 9 divisions for 9 domains. The simulation time for 1, 3 and 9 domains are, respectively 30 min, 80 min and 135 min approximately.

As can be observed in the results of Figs. 10 and 11, the simulated results are in agreement with the measurements. In the worst case, the relative discrepancy was inferior to 8.5%. The force results for simulations with 1, 3 and 9 domains were practically the same, but with only 1 domain the result was calculated almost 4 times faster than in 9 domains. Some small discrepancies were found between simulated and measured results in the region of the minimal values, which can be explained by the fact that the adjustment in the magnetic field presented in Fig. 9 was performed only for the transversal field, neglecting its perpendicular component. Besides, the approximation of the superconducting tape as an isotropic material could have some influence in this small discrepancy.

In Fig. 12 it is shown the force generated in two cases: ZFC and FC. In the first case (ZFC), the sample starts to move to right being its leftmost edge at position x = -35 mm (axis in Fig. 3), with the rightmost edge at 5 mm from the MC boarder. In the second case (FC), the sample is cooled down when it is placed at position x = 3.5 mm, just nearly the center of first (from left) pole of the MC. When the stack is moved to right in ZFC case, entering the MC, it starts to be magnetized from the right side. When the stack is displaced, step by step to the right, the magnetized zone increases and at the same time starts its magnetization cycling under the cycling field, pole by pole, generating the force profile shown in Fig. 12. In this case the force is increased when the stack penetrates in the MC, at a constant level when it is fully inside, and decreasing when exiting the MC.

In a FC process, when the stack is cooled down, the force is zero. The magnetic field is fully trapped by the stack. When moving to the right, the stack, now fully magnetized, is subjected to the oscillating field, starting each part to be cycled accordingly with its hysteretic properties. The force developed changes according to the interaction at the edges, leading to the curve shown in Fig 12. It is worth to remark that the coincidence of the profiles when both samples are fully inside the MC, only can occur if both are identically magnetized. This fact points out that the ZFC magnetization process has achieved the saturation as expected taking in account the flux density of the field applied.

After comparing the simulated results with some experiments, the model was extrapolated to investigate some specific parameter influence in the results, keeping all the other parameters fixed. The first parameter that was investigated was the n exponent in the power law, as presented in Fig. 13. For those simulations the critical current is 270 A and the speed was 0.344 mm/s. It is possible to note that stacks made with 2G tapes having a smaller n exponent can have a slightly higher force. Fig. 13 presents in its detail the normalized mean force results in relation with the mean force for n = 10. The mean force here was calculated considering all the values between x = 0 mm and 25 mm. Compared with the n = 10, the mean force had a decay of almost 8 %. It should be also considered that the dependence with n is very weak, as shown in Fig. 13. It is well stated that a change of n from 20 to 50 affects in less than a 3 % the force. It is also relevant to take into account that the measurement of the n value is somewhat noisy due to the weak dependence of most of the measurements available with n when its value is larger than 20. Also we should consider that n measured in coated conductors is not an intrinsic parameter of the superconducting material because the stabilizing layers, as copper or silver, cooperate in the electrical transport just in the transition.

It should be noted that the fluctuation in the force is an effect of the sample size, which is smaller than the MC length and generates different magnetic interaction in the edges. If the sample was much larger than the magnetic field periodic region, it would be expected a constant force for each speed.

Fig. 14 presents the simulated force results for tapes with several critical current values, n = 35 and v = 0.344 mm/s. By this figure, it seems that the force varies linearly with critical current. This information can be confirmed by Fig. 15, which shows the normalized mean force result in relation with the mean force result for a critical current of 150 A.

The influence of the relative speed between the 2G tape stack and the travelling magnetic field in the force result was also investigated. For a critical current of 281 A and n = 35, the force was calculated in the stack for several speeds of the traveling magnetic field, starting at 0.5 mm/s and a maximum velocity of 50.0 mm/s, as presented in Fig. 16.

Previously, Figs. 10 and 11 have shown the agreement between experimental and simulated force results for two different speeds. For this reason, the simulated results have been extrapolated for a large range of speeds, as presented in Fig. 16.

In Fig. 17 it can be checked that the behavior is in both cases logarithmic, but with different slopes. In fact, it could be an experimental method to determine the n value of a sample measuring the forces as function of the velocities. From the physical point of view this behavior can be attributed to the flux creep effect, since at higher speeds the time for the flux relaxation is smaller and the force do not decay so much.

V. Conclusion

A novel configuration for a linear superconducting motor was presented in this manuscript. This motor is composed by a stator, which produces a traveling magnetic field wave and a stack of second generation (2G) tapes. The main motivation for this work was to investigate the feasibility of this kind of linear motor.

A simple experiment was proposed to measure the produced magnetic force in a 2G tape stack due to an external coherent multipolar magnetic field passing through it. In order to achieve the desired external magnetic field profile, several Nd-Fe-B permanent magnets and soft ferromagnetic bars were used. Two stepper motors control the relative movement between the 2G stack and the external field, while a load cell measures the force. By the presented results a mean force density of about 5 N/g was obtained for this kind of machine. This value is much higher than the force density achieved in conventional linear motors.

Experimental results were compared with 2D simulations using H-formulation implemented by FEM, leading to a maximum

relative error of 8.5%. The model was extrapolated and some parameters were changed to investigate their influence into the force. It was observed that the *n* exponent has small influence on the force. Also, this force was higher for smaller values of *n*. The simulated force increases linearly with the 2G tape critical current. Finally, it was observed a logarithmic dependence between the force and the traveling field speed.

By the simulated and measured results, it can be concluded that 2G tape stacks have potential to be used in superconducting electric linear motors. Furthermore, the applied model can be used in order to scale up the superconducting linear motor to several applications. An estimated force density of almost 500 N/kg was obtained for the displacer. This value is much higher than any technology found in the literature.

VI. Acknowledgments

The authors would like to thank the Brazilian Agency CNPq for the grant “Science without Borders” and the financial supported given by the: European Union agencies for the FORTISSIMO project FP7-2013-ICT-609029, EUROTAPES project FP7-NMP-Large-2011-280432, Eurofusion project PPPT-WPMAG 2014, and EU COST ACTIONS MP1201 and MP1014; Spanish Government agencies for Severo Ochoa Programme Centres of Excellence in R&D (SEV-2015-0496), CONSOLIDER Excellence Network (MAT2015-68994-REDC) and project MAT2014-56063-C2-1-R; Catalan Government for 2014-SGR-753.

VII. References

[1] P. J. Costa Branco, R. Almeida and J. A. Dente, "On Using Meissner Effect to Conceive a New Linear Electromagnetic Launcher by Zero-Field-Cooling YBCO Bulk Superconductors," in IEEE Transactions on Industrial Electronics, vol. 61, no. 11, pp. 5894-5902, Nov. 2014. doi: 10.1109/TIE.2014.2316246.

[2] R. Moulin, J. Leveque, L. Durantay, B. Douine, D. Netter and A. Rezzoug, "Superconducting Multistack Inductor for Synchronous Motors Using the Diamagnetism Property of Bulk Material," in IEEE Transactions on Industrial Electronics, vol. 57, no. 1, pp. 146-153, Jan. 2010. doi: 10.1109/TIE.2009.2034284.

[3] A. B. Abrahamsen *et al.*: “Superconducting wind turbine generators,” Superconductor Science and Technology, v. 23, n. 3, p. 034019, 2010. DOI: 10.1088/0953-2048/23/3/034019.

[4] Y. Itoh *et al.*: “High-temperature superconducting motor using Y-Ba-Cu-O bulk magnets,” *Japanese Journal of Applied Physics*, v. 34, n. 10R, p. 5574, 1995. DOI: 10.1143/JJAP.34.5574.

[5] H. Matsuzaki *et al.*: “An axial gap-type HTS bulk synchronous motor excited by pulsed-field magnetization with vortex-type armature copper windings,” IEEE Transactions on Applied Superconductivity, vol. 15, no. 2, pp. 2222-2225, June 2005. DOI: 10.1109/TASC.2005.849617.

[6] Y. JIANG *et al.*: “The design, magnetization and control of a superconducting permanent magnet synchronous motor,” *Superconductor Science and Technology*, v. 21, n. 6, p. 065011, 2008. DOI: 10.1088/0953-2048/21/6/065011.

[7] A. Patel, S.C. Hopkins and B.A. Glowacki; “Trapped fields up to 2 T in a 12 mm square stack of commercial superconducting tape using pulsed field magnetization,” *Superconductor Science and Technology*, v. 26, n. 3, p. 032001, 2013. DOI: 10.1088/0953-2048/26/3/032001.

[8] T.B. Mitchell-Williams *et al.*: “Uniform trapped fields produced by stacks of HTS coated conductor tape”, *Superconductor Science and Technology*, 29 (8), art. no. 085008, 2016. DOI: 10.1088/0953-2048/29/8/085008.

[9] S. Zou et. al.: “Simulation and experiments of stacks of high temperature superconducting coated conductors magnetized by pulsed field magnetization with multi-pulse technique”, Superconductor Science and Technology, 30 (1), art. no. 014010, 2017, DOI: 10.1088/0953-2048/30/1/014010.

[10] A. Augieri et al., "Electrical Characterization of ENEA High Temperature Superconducting Cable," in IEEE Transactions on Applied Superconductivity, vol. 25, no. 3, pp. 1-4, June 2015. doi: 10.1109/TASC.2014.2364391

[11] W. H. Fietz, M. J. Wolf, A. Preuss, R. Heller and K. P. Weiss, "High-Current HTS Cables: Status and Actual Development," in IEEE Transactions on Applied Superconductivity, vol. 26, no. 4, pp. 1-5, June 2016. doi: 10.1109/TASC.2016.2517319

[12] M. Takayasu, L. Chiesa, L. Bromberg, J.V. Minervini: “HTS twisted stacked-tape cable conductor”, Superconductor Science and Technology, 25 (1), art. no. 014011, 2012, DOI: 10.1088/0953-2048/25/1/014011

[13] M. Takayasu, L. Chiesa, N. C. Allen and J. V. Minervini, "Present Status and Recent Developments of the Twisted Stacked-Tape Cable Conductor," in IEEE Transactions on Applied Superconductivity, vol. 26, no. 2, pp. 25-34, March 2016. doi: 10.1109/TASC.2016.2521827

[14] M. Baghdadi, H. S. Ruiz, J. F. Fagnard, M. Zhang, W. Wang and T. A. Coombs, "Investigation of Demagnetization in HTS Stacked Tapes Implemented in Electric Machines as a Result of Crossed Magnetic Field," in IEEE Transactions on Applied Superconductivity, vol. 25, no. 3, pp. 1-4, June 2015. doi: 10.1109/TASC.2014.2372873

[15] A. Patel, A. Baskys, S. C. Hopkins, V. Kalitka, A. Molodyk and B. A. Glowacki, "Pulsed-Field Magnetization of Superconducting Tape Stacks for Motor Applications," in IEEE Transactions on Applied Superconductivity, vol. 25, no. 3, pp. 1-5, June 2015. doi: 10.1109/TASC.2015.2389142

[16] F. Sass, D. H. N. Dias, G. G. Sotelo and R. de Andrade Jr.: "Superconducting Levitation Using Coated Conductors," in IEEE Transactions on Applied Superconductivity, vol. 23, no. 3, pp. 3600905-3600905, June 2013. doi: 10.1109/TASC.2012.2234172

[17] Sass, F., Sotelo, G.G., De Andrade, R., Sirois, F.: “H-formulation for simulating levitation forces acting on HTS bulks and stacks of 2G coated conductors”, Superconductor Science and Technology, 28 (12), art. no. 125012, 2015. DOI: 10.1088/0953-2048/28/12/125012

[18] Patel, A., Hopkins, S.C., Baskys, A., Kalitka, V., Molodyk, A., Glowacki, B.A.: “Magnetic levitation using high temperature superconducting pancake coils as composite bulk cylinders”, Superconductor Science and Technology, 28 (11), art. no. 115007, 2015. DOI: 10.1088/0953-2048/28/11/115007

[19] F. Sass *et al.*: “Persistent currents in a magnetic bearing with coated conductors,” *Journal of Applied Physics*, v. 118, n. 20, p. 203901, 2015. DOI: 10.1063/1.4936178.

[20] Chapman, Stephen. Electric machinery fundamentals. Tata McGraw-Hill Education, 2005.

[21] Werfel, F. N., et al. "Superconductor bearings, flywheels and transportation." Superconductor Science and Technology 25.1 (2011): 014007.

[22] Z. Hong, A. Campbell and T. Coombs: “Numerical solution of critical state in superconductivity by finite element software,” Supercond. Sci. Technol., vol. 19, no. 12, pp. 1246-1252, 2006, DOI: 10.1088/0953-2048/19/12/004.

[23] R. Brambilla, F. Grilli and L. Martini: “Development of an edge-element model for AC loss computation of high-temperature superconductors,” Supercond. Sci. Technol., vol. 20, no. 1, pp. 16-24, 2007, DOI: 10.1088/0953-2048/20/1/004.

[24] V. Zermeno et. al.: “Calculation of alternating current losses in stacks and coils made of second generation high temperature superconducting tapes for large scale applications,” Journal of Applied Physics, vol. 114, pp. 173901, 2013, DOI: 10.1063/1.4827375.

[25] F. Sass et. al.: “H-formulation for simulating levitation forces acting on HTS bulks and stacks of 2G coated conductors,” Supercond. Sci. Technol., vol. 28, no. 12, pp. 125012, 2015, doi:10.1088/0953-2048/28/12/125012.
[26] G. G. Sotelo *et al.*: “H-Formulation FEM Modeling of the Current Distribution in 2G HTS Tapes and Its Experimental Validation Using Hall Probe Mapping,” IEEE Transactions on Applied Superconductivity, vol. 26, no. 8, pp. 1-10, Dec. 2016. DOI: 10.1109/TASC.2016.2591825.
[27] G. Nishijima, H. Kitaguchi, S. Awaji and H. S. Shin: “Transport property measurement of practical coated conductor with copper stabilizer,” In AIP Conference Proceedings, vol. 1435, n. 1, pp. 258-264, 2012. DOI: 10.1063/1.4712104.
[28] W. Haynes, *CRC Handbook of Chemistry and Physics* 95th Ed., 2015, CRC Press.
[29] J. Lu, E. S. Choi and H. D. Zhou: “Physical properties of Hastelloy® C-276™ at cryogenic temperatures,” *Journal of Applied Physics*, vol. 103, no. 6, pp. 064908, 2008, DOI: 10.1063/1.2899058.
[30] R. A. H. Oliveira et al: “Evaluation of linear induction motors with two different topologies by FEM,” *10th International Symposium on Linear Drives for Industry Application* (LDIA'2015), Aachen, 2015.
[31] H. M. Hasanien, A. S. Abd-Rabou and S. M. Sakr: “Design optimization of transverse flux linear motor for weight reduction and performance improvement using response surface methodology and genetic algorithms,” *IEEE Transactions on Energy Conversion*, vol. 25.3, pp. 598-605, 2010.
[32] D. Wang et al: “Design, Optimization and Prototyping of Segmental Type Linear Switched Reluctance Motor with a Toroidally Wound Mover for Vertical Propulsion Application,” IEEE Transactions on Industrial Electronics, accepted for publication, 2017, DOI: 10.1109/TIE.2017.2740824.
[33] N. S. Lobo, H. S. Lim and R. Krishnan: “Comparison of Linear Switched Reluctance Machines for Vertical Propulsion Application: Analysis, Design, and Experimental Correlation,” *IEEE Transactions on Industry Applications*, vol. 44, no. 4, pp. 1134-1142, 2008. DOI: 10.1109/TIA.2008.926294

Figures:

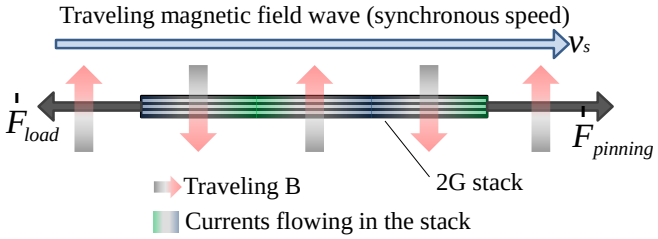

Fig. 1. Traveling magnetic field and a superconducting 2G stack.

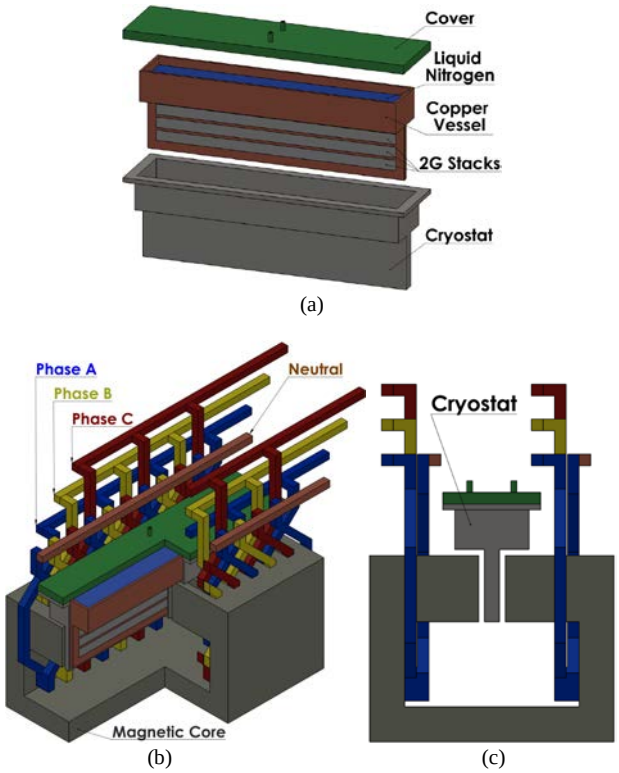

Fig. 2. Schematic of the proposed linear motor: (a) Exploded view of the cryostat, (b) Isometric view with cuts of the three phase stator and cryostat, (c) Frontal view of the linear motor.

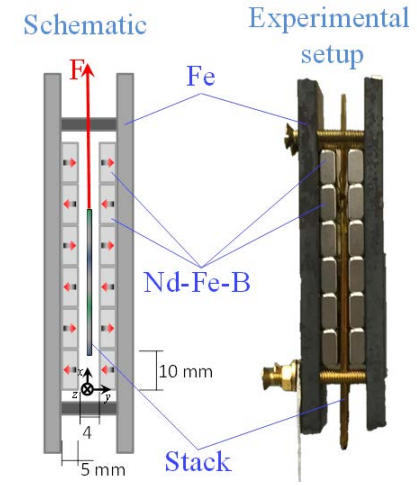

Fig. 3. Schematic and photo of the experimental rig, with the external field and the 2G stack.

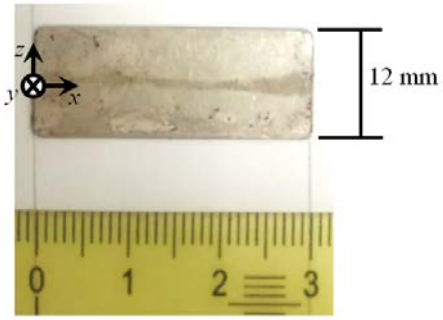

Fig. 4. 2G tape stack constructed for this experiment.

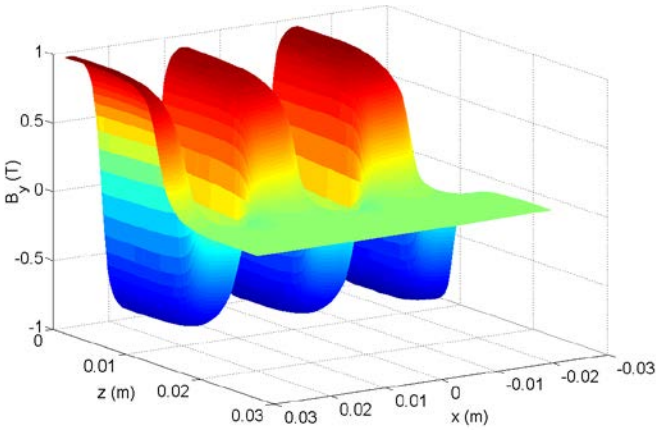

Fig. 5. Transversal component of the magnetic flux density in the gap region.

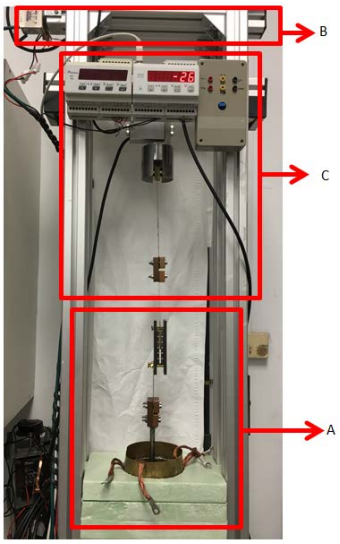

Fig. 6. Experimental rig to measure the force between the 2G tape stack and the external magnetic field.

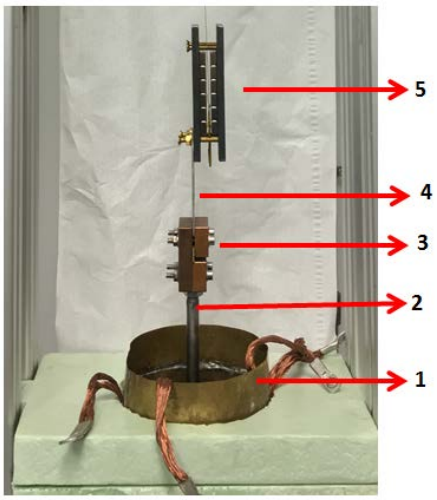

Fig. 7. Detailed part A of the experimental rig (Fig. 6). The stack movement is along x direction (Figs. 3 and 4).

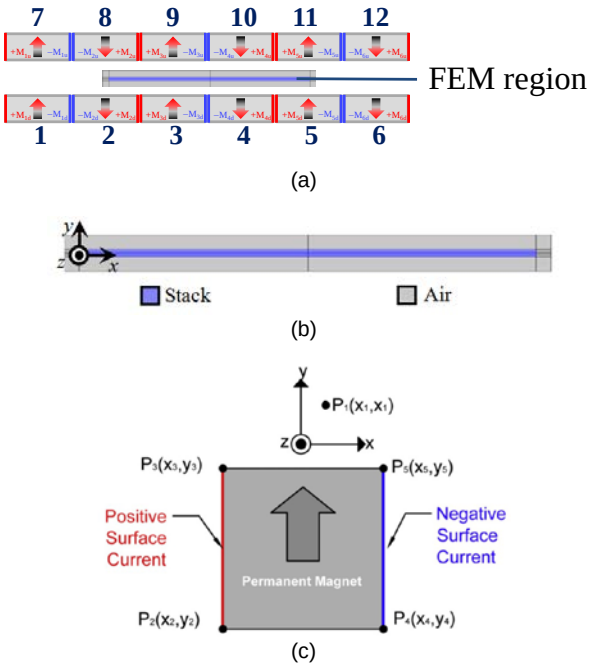

Fig. 8. (a) Schematic of the external currents to permanent magnets modeling. (b) FEM region and domains used in the simulations. (c) Current representation for an individual permanent magnet.

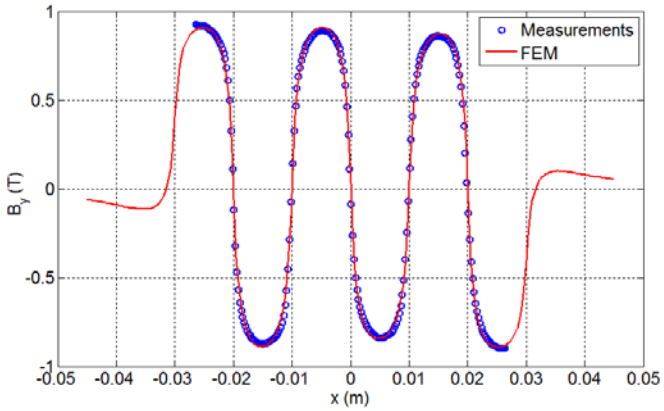

Fig. 9. Comparison between simulated and measured results for the magnetic induction.

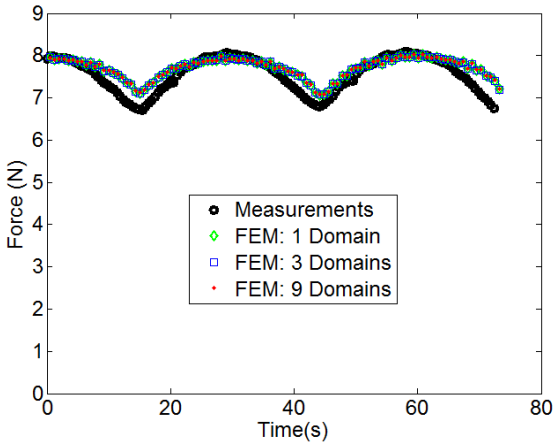

Fig. 10. Simulated and measured force results for v = 0.344 mm/s.

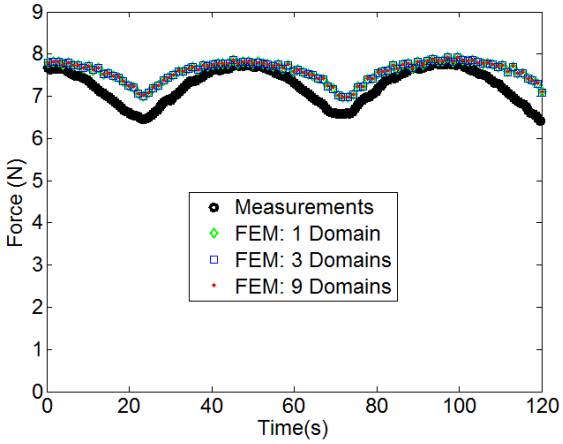

Fig. 11. Simulated and measured force results for v = 0.207 mm/s.

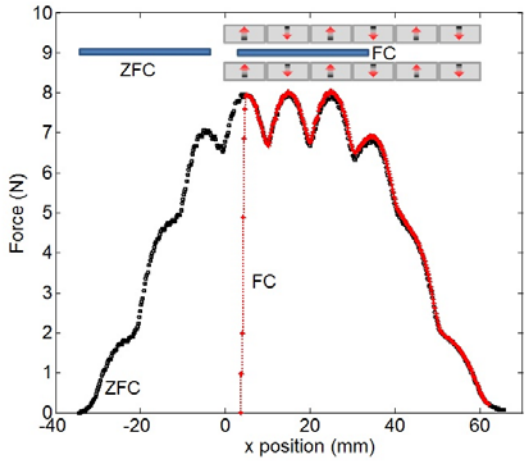

Fig. 12. Measured force results for v = 0.344 mm/s in different cooling procedures. The initial position is presented in detail.

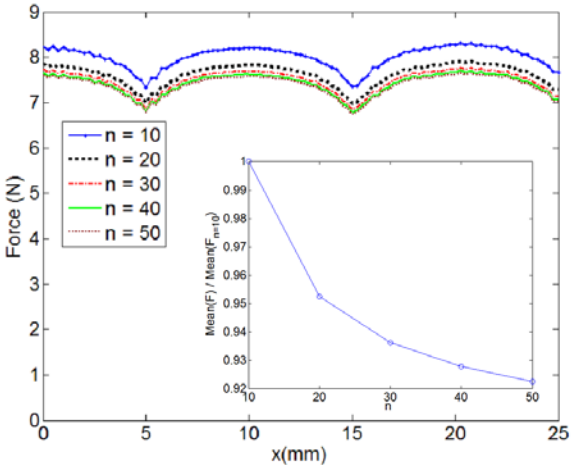

Fig. 13. Simulated results for different *n* exponents. In detail the normalized mean value of the force in relation with the mean value of the force for *n* = 10.

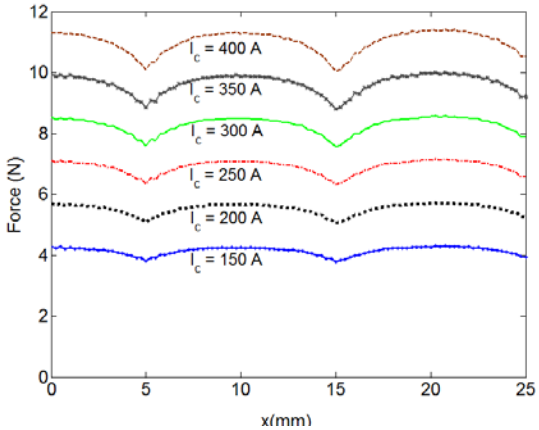

Fig. 14. Simulated results for different critical currents.

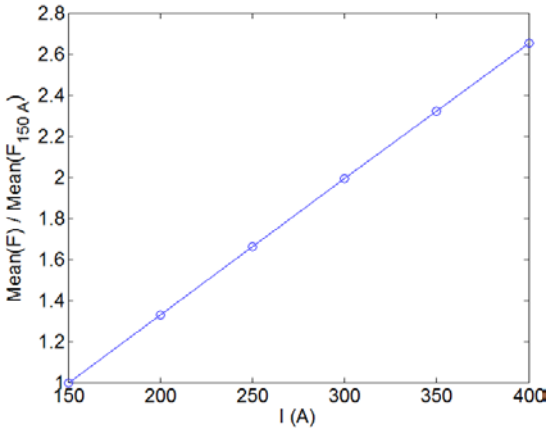

Fig. 15. Normalized mean value of the force in relation with the mean value of the force for Ic =150 A.

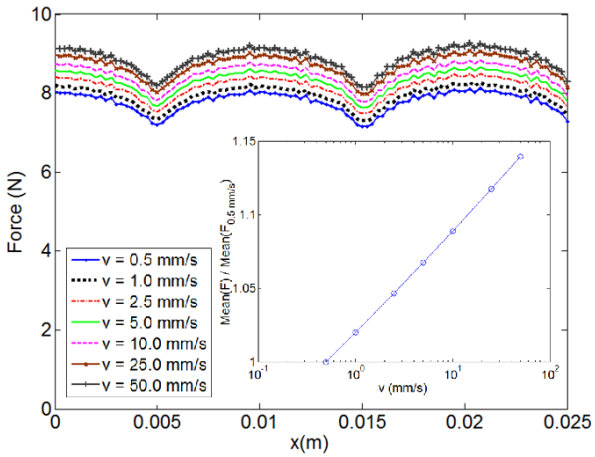

Fig. 16. Simulated results for different relative speeds. In detail, the normalized mean value of the force in relation with the mean value of the force for v =0.5 mm/s.

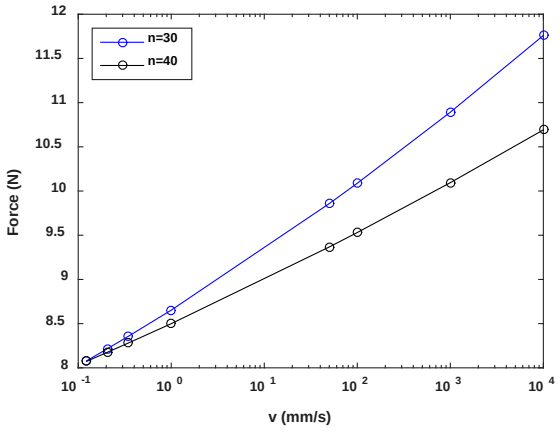

Fig. 17. Maximum value of the force in front of logarithm of velocity.

TABLES

TABLE I
PARAMETERS OF THE 2G TAPES AND THE STACK.

Parameters for the 2G tape	*Value*
Width	12 mm
HTS thickness	1 μm
Silver thickness	2 μm
Substrate (Hastelloy C-276) thickness	50 μm
Tape total thickness	55 μm
Critical current measured, self-field @ 77K (1 μV/cm)	281 A
Power-law parameter *n* (by fitting with the measurements)	35
Silver resistivity [28]	2.7 nΩ·m
Hastelloy C-276 resistivity [29]	1.25 μΩ·m
Parameters for the Stack	***Value***
Width	12 mm
Total thickness (9 layers)	510 μm
Length	30 mm
Mass	1.48 g

TABLE II
FORCE DENSITY COMPARISON AMONG SEVERAL LINEAR MOTORS.

Type of linear motor	Displacer mass (kg)	Traction Force (N)	Force density (N/kg)
HTS with stack	4.5	2240	497.77
Induction 1 [30]	132	2403	18.20
Induction 2 [30]	46	910	19.78
Transverse flux - PM [31]	8.38	742	88.54
Switched reluctance [32]	1.63	47.28	29.00
Switched reluctance [33]	6.5	180	27.69